



# A Search for Analogs of KIC 8462852 (Boyajian’s Star): A Proof of Concept and the First Candidates

Edward G. Schmidt<sup>1</sup> Department of Physics and Astronomy, University of Nebraska, Lincoln, NE, USA; [eschmidt1@unl.edu](mailto:eschmidt1@unl.edu)*Received 2019 June 24; revised 2019 July 1; accepted 2019 July 2; published 2019 July 18*

## Abstract

The seemingly normal F dwarf, KIC 8462852 (a.k.a. Boyajian’s Star), has been observed to exhibit two types of behavior unique among known variable stars: infrequent episodes of small brightness dips and a long-term decline in brightness between the dips. No satisfactory mechanism has been found for this behavior, at least in part, because there is only one known example. To begin to rectify this, we have searched for other stars exhibiting similar dipping behavior using the Northern Sky Variability Survey and have used data from the All Sky Automated Survey for Supernovae to further investigate the behavior. Twenty-one stars are identified as possible dippers. Fifteen may be similar to Boyajian’s star and the other six are likely to be more extreme examples of the same phenomenon. Using data from the *Gaia* Second Data Release we show that the dipper candidates are located in two restricted regions of the H-R diagram, near the main sequence with masses near 1 solar mass and in the red giant region near the evolutionary track for 2 solar mass stars. Stars in the former group are considered to be likely analogs to Boyajian’s star and should be studied in more detail to gain insights into the dipping phenomenon.

*Key words:* stars: peculiar – stars: variables: general

## 1. Introduction

Citizen scientists from the Planet Hunters Project noted unusual dips widely scattered across the 1460 days of the *Kepler* mission light curve of the star KIC 8462852, a.k.a. Boyajian’s star<sup>2</sup> (Boyajian et al. 2016). These were followed almost 1500 days (four years) later by another group of overlapping dips (Boyajian et al. 2018). The dips were typically a few days to a week in duration and were often in groups that lasted as long as several months. Their depths ranged from 0.5% to 22% of the continuum level.<sup>3</sup> While the star appears to be quite constant between the dipping events a number of authors, beginning with Schaefer (2016), have claimed to find long-term dimming at wavelengths from the ultraviolet to the infrared. These behaviors are unprecedented among known variable stars.

Boyajian et al. (2016) thoroughly investigated this star. They found it to be a typical F3V star with no apparent spectral peculiarities. It lacks an infrared excess and has no companion. Pre-main-sequence stars often exhibit dips along with several other types of variability (Cody et al. 2014), but the star’s near constancy between the dips and lack of an infrared excess indicate that it is not a young star.

A variety of explanations have been proposed for the unusual behavior of Boyajian’s star. These include variations within the star itself, occultations by clumps of dust or other objects orbiting the star and even variations in the interstellar medium. However, no fully satisfactory model has yet been proposed. The reader is referred to Boyajian et al. (2018) and

Bodman et al. (2018) for much more exhaustive reviews of studies related to this star.

Follow-up observations of Boyajian’s star continue and will no doubt provide further insights into the physics behind its behavior. However, as long as it remains the unique example, it will be difficult to arrive at a full understanding of the mechanisms at work or to assess its broader importance to stellar astrophysics. This paper reports a first attempt to find other similar stars using data from large photometric surveys that are now available. I am publishing the list of the first stars discovered now to encourage those with access to suitable instrumentation to undertake follow-up observations. Further lists will be published as I explore this area further.

## 2. The Search

The Northern Sky Variable Survey (NSVS; Wozniak et al. 2004) was used to search for candidates and the All Sky Automated Survey for Supernovae (ASAS-SN; Shappee et al. 2014; Kochanek et al. 2017) to further filter the candidates and to provide information on their long-term behavior.

The NSVS Public Data Release<sup>4</sup> consists of the subset of photometric data from the ROTSE-1 survey (Akerlof et al. 2000) taken from 1999 April to 2000 March (Julian dates from 2,451,273 to 2,451,630). For the purpose of covering the entire sky, the celestial sphere was covered by two hundred six  $16^\circ \times 16^\circ$  tiles. Each tile was imaged by four cameras, designated A, B, C, and D, with  $8.2 \times 8.2$  fields. For most of the observations two frames were taken back-to-back at each setting of the telescope. Under favorable conditions fields were visited twice in a night. The data release contains light curves for about 14 million objects.

To assess the suitability of the NSVS for our search, we calculated the intervals between successive light-curve points for a sample of stars from the survey. In doing this, back-to-back pairs of magnitudes were treated as a single observation.

<sup>1</sup> Retired. Mailing address: 685 S. La Posada Circle #3301, Green Valley, AZ 85614, USA.

<sup>2</sup> We will follow Wright & Sigurdsson (2016) in referring to this object as “Boyajian’s star,” to the decreases in brightness with durations of days as “dips” and dimming (or brightening) over intervals of years as “long-term dimming” (brightening).

<sup>3</sup> We shall refer to the level of the quiescent intervals between dips as the “continuum.”

<sup>4</sup> Available at <http://skydot.lanl.gov/>.

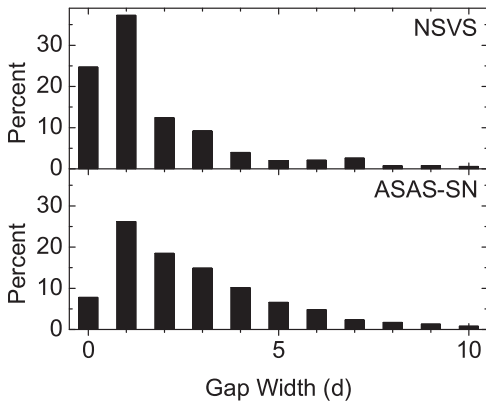


**Figure 1.** Distributions of the widths of the light-curve gaps from NSVS (upper panel) and ASAS-SN (lower panel).

The top panel in Figure 1 shows the resulting distribution of these light-curve gaps. Those that are less than half a day long, the first bar, represent nights with more than one visit while the gaps between 0.5 and 1.5 days, the second bar, are instances where the same star was observed on successive nights. The significant number of repeated observations on a single night and on successive nights are important for finding relatively narrow dips. Thus, the NSVS is a suitable survey for this search.

The ASAS-SN utilizes 20 small telescopes widely distributed around the globe. The original goal was to scan the sky to detect bright transients with a particular emphasis on nearby supernovae. Unlike other surveys, the data are made available on a star-by-star basis as soon as they are obtained.

In the lower panel of Figure 1 we show the histogram of the gap widths for the ASAS-SN data. Generally, at each setting of the telescope several exposures were taken in succession to provide dither sets. Again, each dither set was treated as a single observation. There are only about one-third as many nights with multiple observations and fewer with observations on successive nights than was the case with the NSVS data. This will cause more dips to be missed making the ASAS-SN less suitable for the initial search. Nonetheless, the longer time span of the observations (between  $2\frac{2}{3}$  and nearly 6 yr) make this a useful source of information with which to explore the long-term behavior of the candidates.

These surveys are not at all comparable to the *Kepler* survey with its four dozen data points per day, nearly continuous 1500 day span, and millimagnitude accuracy. As a result our search will produce a woefully incomplete sample. However, it will identify interesting stars for further study and will give us a first look at what sort of stars exhibit dipping behavior.

### 2.1. Identification of Candidates

We searched a region of the NSVS defined by tiles 23–26, 41–45, and 62–67 (see Figure 1 of Akerlof et al. 2000 for the locations of the tiles). This region is centered at  $\alpha = 20:08$ ,  $\delta = +45:00$  and has a total area of approximately 2980 square degrees. It includes the *Kepler* field.

In presenting the NSVS, Wozniak et al. (2004) identified individual measurements as “good” based on processing flags. We have omitted measurements that failed their criteria as well as measurements with listed magnitude errors greater than 0.10

mag from the following analysis. In the search and the plotted light curves, we have treated members of back-to-back pairs as independent observations.

A computer code was developed to screen the NSVS data for a preliminary set of candidates. For each star, it calculated the median magnitude and standard deviation from all of the magnitudes, then trimmed the sample at three standard deviations and recomputed the median and the standard deviation. These values were adopted as the continuum magnitude,  $m_{\text{cont}}$ , and the standard deviation about it,  $\sigma_{\text{cont}}$ .

The light curves were then searched for points more than  $3\sigma_{\text{cont}}$  fainter than  $m_{\text{cont}}$ . Stars with at least one dip consisting of five or more contiguous low points no deeper than 0.75 mag were selected for visual inspection; about 200 stars out of the 2.3 million in our field were selected.

In the inspection we rejected stars using the following criteria in this order:

1. Any star with an NSVS light curve that resembled a possible eclipsing binary was rejected. This included any stars with dips wider than a few days and stars with regularly spaced minima.
2. Any star with an NSVS light curve resembling an intrinsic variable was rejected.
3. Finding charts were downloaded from the NASA/IPAC Infrared Science Archive website.<sup>5</sup> The NSVS coordinates for some stars were found to be nearly centered between two (or occasionally more) close stars. This indicates that the NSVS object is a blend of stars so such objects were rejected.
4. Light curves for the remaining stars were downloaded from the ASAS-SN website.<sup>6</sup> At the time of the downloads, data extended from JD 2,455,955 until 2,458,184, although individual stars cover shorter intervals. These were examined by eye and, as in 1 and 2, any star with a light curve that appeared to be an eclipsing binary or intrinsic variable was rejected.

In applying these criteria, we favored rejection in dubious cases so as to keep the final sample as free as possible of false positives.

Twenty-one stars remained after the manual inspection. Table 1 lists these objects. The first column gives the NSVS number of each star while the sexagesimal designation is given in column 2.

As described above, we required that a dip be defined by at least five contiguous data points to qualify a star as a possible object of interest. However, in many cases other dips with fewer points (generally a single point)  $3\sigma$  below the continuum are visible in the NSVS light curve. Column 3 lists the total number of dips including the one that was used to identify the star as a candidate. Column 4 gives the depth below the continuum of the deepest dip. The remaining columns are described below.

We have also included Boyajian’s star in Table 2 for comparison with our candidates. Note that no dips were detected during the year of the NSVS coverage.

<sup>5</sup> <https://irsa.ipac.caltech.edu/irsvIEWER/>

<sup>6</sup> <https://asas-sn.osu.edu/>

**Table 1**  
The Dipper Candidates

NSVS Number (1)	Sexagesimal Designation (2)	NSVS		ASAS-SN					Note (10)
		$N_{\text{dips}}$ (3)	$D_{\text{max}}$ (4) mag	$N_{\text{dips}}$ (5)	$D_{\text{max}}$ (6) mag	$N_{\text{humps}}$ (7)	$T_{\text{obs}}$ (8) days	$R_{\text{dips}}$ (9) $\text{yr}^{-1}$	
Candidates									
2913753	J172435.00+591214.9	1	0.31	4	0.39	3	1380	1.1	a, b
2958269	J174644.74+645345.5	2	0.16	0	...	4	1600	0.0	a
3037513	J183842.27+540758.2	2	0.11	10	0.06	3	1290	2.8	a, b
3093586	J194938.87+552016.7	2	0.34	2	0.04	0	1000	0.7	a
3212541	J195855.75+573054.1	2	0.27	24	0.43	0	1030	8.5	c
3242277	J203754.32+542954.0	7	0.38	32	0.37	0	765	23.9	c
5334181	J171722.27+412332.9	3	0.21	1	0.04	2	1160	0.3	a
5436225	J182040.72+455432.2	1	0.21	2	0.10	1	1210	0.6	a
5482005	J182701.22+414742.8	2	0.24	4	0.10	2	1080	1.4	a
5736209	J202717.24+375628.3	3	0.54	26	0.24	0	710	13.4	b, c
7971210	J165847.61+274353.1	2	0.16	0	...	1	1380	0.0	a
8046240	J173720.53+365816.2	1	0.29	3	0.06	1	1340	0.8	a
8128754	J180257.82+271225.8	2	0.14	2	0.17	1	1300	0.6	a
8233191	J184259.67+340332.4	1	0.21	0	...	1	1020	0.0	a
8491743	J201540.61+323416.9	4	0.95	0	...	1	720	0.0	a
8562896	J203219.51+273942.7	6	0.51	27	0.59	0	710	13.9	b, c
8816108	J221236.58+265508.0	2	0.34	2	0.43	2	1210	...	c
8923588	J225015.91+372227.3	4	0.24	25	0.26	0	1080	8.4	c
8935719	J222514.73+270857.7	2	0.33	1	0.06	3	1350	0.3	a
8942941	J223158.12+282442.7	2	0.20	0	...	2	1140	0.0	a, b
8987978	J232054.32+252557.5	1	0.26	5	0.18	3	1340	1.4	a
Boyajian's Star									
5711291	J200615.45+442724.8	0	...	1	0.06	1	951	0.4	a

#### Notes.

<sup>a</sup> Slow dippers.

<sup>b</sup> There is a faint companion within  $20''$  of the program star.

<sup>c</sup> Rapid dippers.

<sup>d</sup> Numerous, often overlapping, dips.

## 2.2. Follow-up

In addition to the data for the candidates themselves, we downloaded data from the ASAS-SN for two stars near each candidate to serve as controls.

With each magnitude, the website provides several quality indicators including the limiting magnitude for a  $5\sigma$  detection. To eliminate data that were affected by high sky brightnesses, we rejected measurements where the stellar magnitude was less than 1.5 mag brighter than the limiting magnitude. It was noted that this parameter correlates well with the estimated photometric errors.

The continuum magnitudes,  $m_{\text{cont}}$ , and the standard deviations of the points relative to it,  $\sigma_{\text{cont}}$ , were determined as described in Section 2.1, and differential magnitudes were formed for each candidate relative to the control stars.

We plotted the original magnitudes and the differential magnitudes against Julian Date and visually examined them for dips. We regarded any data point that fell more than three standard deviations below the continuum in the magnitude plot and was reasonably low in the differential magnitude plots (taking into account the larger scatter in some of them) to be a dip. For each star we have listed the number of such dips in column 5 of Table 1 while column 6 contains the depth of the deepest one.

There is some evidence of short term brightness humps following dips in the light curve of Boyajian's star (e.g., see Figure 2 of Boyajian et al. 2018). For completeness, we have

listed the number of points that lie at least  $3\sigma$  above the continuum in column 7.

The temporal coverage of the light curves is critical to how many dipping events are detected. We have given the duration of continuous temporal coverage in the ASAS-SN,  $T_{\text{obs}}$ , in column 8 of Table 1. Essentially this is the elapsed time over which a star was observed minus seasonal gaps.  $T_{\text{obs}}$  ranges from 710 to 1600 days. The rate of dips,  $R_{\text{dips}} = N_{\text{dips}}/T_{\text{obs}}$ , is tabulated in column 9. Column 10 contains references to footnotes to the table.

## 3. Discussion

### 3.1. The Photometric Behavior

The stars in Table 1 fall into two distinct categories based on the ASAS-SN photometry. The largest category consists of stars with narrow dips (less than a few days wide) and dipping rates,  $R_{\text{dips}}$ , less than three. These stars are identified by footnote a and will be referred to here as ‘‘slow dippers.’’ A second category also has narrow dips but values of  $R_{\text{dips}}$  greater than eight; they are identified by footnote b and will be referred to as ‘‘rapid dippers.’’

#### 3.1.1. Slow Dippers

Fifteen of our candidates, as well as Boyajian's star, fall in this category. Their NSVS light curves are plotted in Figure 2. The solid line is the continuum level while the dotted line is  $3\sigma_{\text{cont}}$  below it. As indicated by the entries in column 3 of Table 1,

**Table 2**  
Other Properties of the Candidates

NSVS (1)	$V$ (2) (mag)	$\sigma_V$ (3) (mag)	Source <sup>a</sup> (4)	$\pi$ (5) (mas)	$\sigma_\pi$ (6)	$T_{\text{eff}}$ (7) (K)	$\text{Log}(L/L_\odot)$ (8)	Notes (9)
Candidates								
2913753	13.639	0.049	A	4.50	0.4%	4590	−0.65	b, c
2958269	12.778	0.006	A	0.37	9.7%	4588	1.82	b, d
3037513	11.38	0.11	S	1.69	1.2%	5259	0.88	b, c
3093586	12.31	0.01	A	3.01	0.8%	5861	0.02	b, c
3212541	9.61	0.03	S	1.50	3.5%	4782	1.79	e, d
3242277	9.93	0.03	S	0.83	3.4%	8401	...	e, f
5334181	(13.08) <sup>g</sup>	0.04	N	...	...	...	...	b
5436225	12.604	...	G	3.69	0.6%	5232	−0.17	b, c
5482005	12.695	...	G	1.61	1.5%	6580	0.38	b, c
5736209	13.156	0.156	A	0.59	4.0%	3994	1.58	e, d, h
7971210	12.407	0.075	A	1.59	1.5%	5868	0.56	b, c
8046240	12.695	0.05	A	2.44	0.8%	5702	0.11	b, c
8128754	12.193	0.006	A	0.61	4.7%	4126	1.82	b, d
8233191	12.994	0.078	A	0.09	29.2%	...	...	b
8491743	12.141	0.079	A	0.93	2.6%	4104	1.48	b, d
8562896	12.045	0.062	A	3.19	1.2%	5381	0.09	c, e, i
8816108	8.94	0.02	S	2.19	2.4%	4925	1.76	d, e
8923588	11.77	0.013	A	1.72	1.9%	6299	0.74	c, e
8935719	12.59	0.025	A	0.47	7.4%	4708	1.70	b, d
8942941	12.544	0.058	A	0.85	4.3%	5807	1.03	b, c
8987978	12.639	0.037	A	0.44	8.6%	4888	1.70	b, d
Boyajian's Star								
5711291	11.705	0.017	B	2.22	1.1%	5899	0.47	b, c

#### Notes.

<sup>a</sup> A: APASS: the AAVSO Photometric All-Sky Survey, <https://www.aavso.org/apass>; B: Boyajian et al. (2016); G: transformed from *Gaia* photometry using transformations from Evans et al. (2018); N: NSVS; S: SIMBAD Astronomical Database <http://simbad.u-strasbg.fr/simbad/>.

<sup>b</sup> Slow dippers.

<sup>c</sup> In the main-sequence group.

<sup>d</sup> In the red giant group.

<sup>e</sup> Rapid dippers.

<sup>f</sup> NSVS 3242277 is V828 Cyg. It is classified as variable type EB/DM in the VSX with a spectral type of B8. Its effective temperature does not fall near either region of dippers in Figure 4 so we reject it as a candidate.

<sup>g</sup> The magnitude listed for NSVS 5334181 is on the NSVS magnitude system.

<sup>h</sup> NSVS 5736209 is V2544 Cyg. It is classified as variable type EA in the VSX.

<sup>i</sup> NSVS 8562896 is BB Vul. It is classified as variable type EA/RS in the VSX.

nearly two-thirds of them exhibit additional dips (i.e.,  $N_{\text{dips}} > 1$ ), mostly consisting of a single point below the  $3\sigma$  level.

In the ASAS-SN light curves, the dips are almost all composed of a single point and are all well separated. Plots of them do not add any significant information to what is contained in column 5 of Table 1 so they are not presented here. It can be seen from  $N_{\text{dips}}$  that two-thirds of the ASAS-SN light curves exhibit dips.

The total number of dips from both the NSVS and the ASAS-SN photometry is between 1 and 12. Five of the slow dippers did not exhibit any dips in their ASAS-SN light curve. Since the two intervals of dipping in Boyajian's star are separated by 1500 days this is not inconsistent with their being similar to Boyajian's star given that  $T_{\text{obs}}$  for these stars are mostly less than that. We have therefore retained all 15 of the slow dippers as candidates.

Boyajian's star is apparently unique among the more than 150,000 stars observed continuously by *Kepler* (Boyajian et al. 2016).<sup>7</sup> Since we searched among 15 times more stars, the 15

stars we found are not inconsistent with finding one among the *Kepler* sample. Of course, this ignores several important factors including that the *Kepler* stars were selected for particular properties from a much larger sample (the *Kepler* Input Catalog), our search is probably seriously incomplete and the possibility that our sample contains some stars that are not actually related to Boyajian's star.

Clearly long-term monitoring of these stars is needed to establish that some or all of the slow dippers are similar to Boyajian's star. Whatever the outcome of such efforts, these stars promise to provide insights into new astrophysical phenomena.

#### 3.1.2. Rapid Dippers

We have plotted the NSVS and ASAS-SN light curves of the six rapid dippers in in Figures 3(a) and (b). The rapid dipping is obvious in the ASAS-SN observations. It ranges from some stars with many well-separated dips to others with nearly constant dipping activity. It is also evident that the dipping rate varies over time for at least some of the stars. This is especially obvious in NSVS 8816108 where the activity seems to have nearly ceased by the third season of observations. It is uncertain

<sup>7</sup> Lacourse (2016) examined the photometry for another 165,000 stars from the *K2* mission without finding an analog to Boyajian's star. However, *K2* only observed each field for about 84 days so dipping activity in any star could easily have been missed.

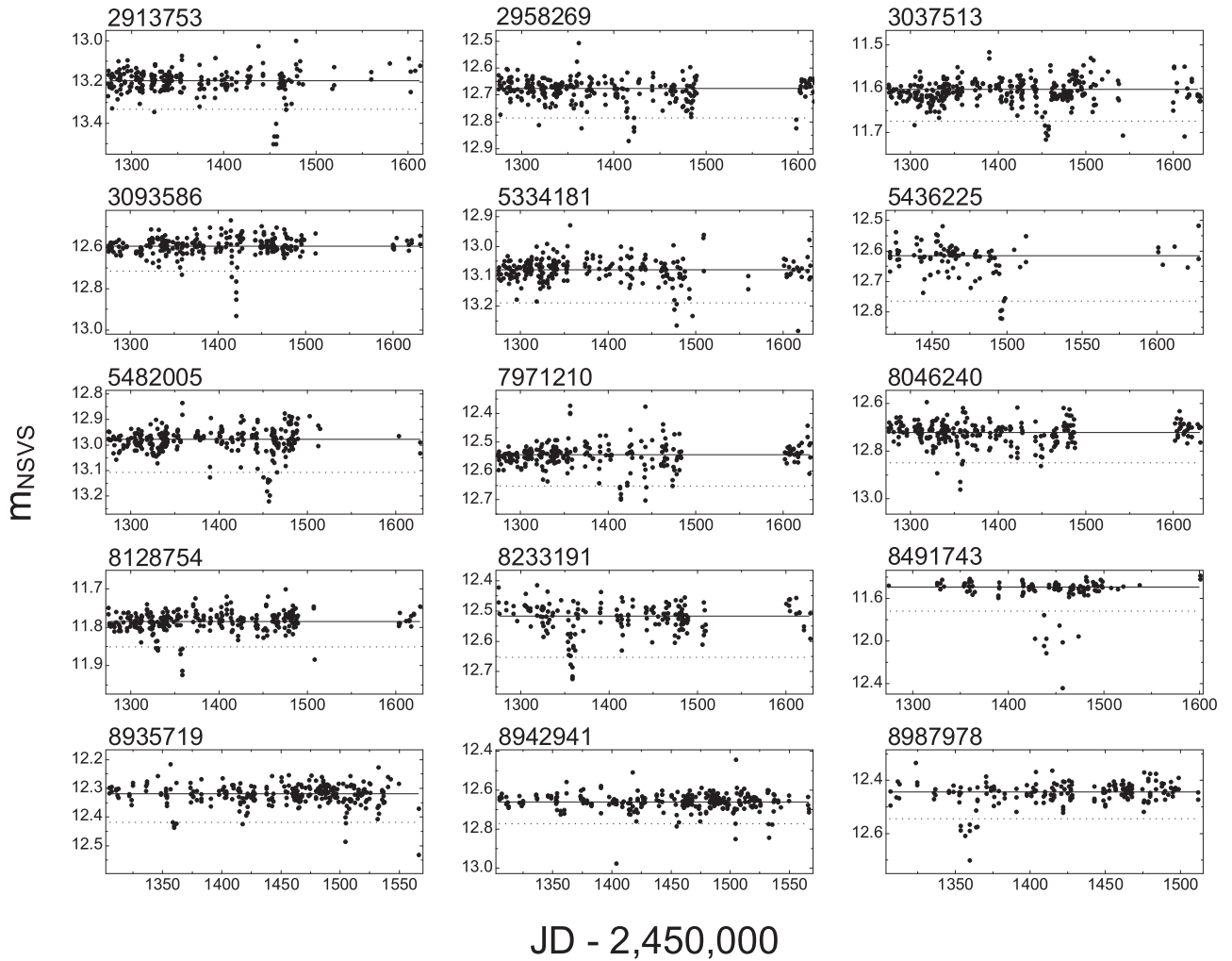


**Figure 2.** NSVS light curves for the stars classified as slow dippers. The solid line is the continuum level and the dashed line is three standard deviations below the continuum.

whether these stars are simply very extreme examples of the behavior of the slow dippers or are a completely different phenomenon

Again, long-term monitoring of these promise to reveal new astrophysical phenomena of interest.

### 3.2. Other Properties

Table 2 presents various properties of our candidates and Boyajian’s star. The first column identifies each star by its NSVS number. Columns 2, 3, and 4 list the  $V$  magnitude, its standard deviation, and the source of the photometry for each star. Columns 5 through 8 give the parallaxes, the errors of the parallaxes, the effective temperatures and the luminosities from the second *Gaia* Data Release (*Gaia* Collaboration 2016, 2018, hereafter *Gaia* DR2). The final column refers to footnotes that give the category from Section 3.1 to which each star belongs and other information discussed below.

Three of the stars, identified by footnotes, are listed in the AAVSO International Variable Star Index<sup>8</sup> as known variables. All three belong to our rapid dipper category and all three are classified as eclipsing binaries in the VSX. For NSVS 5736209 a period of 2.0937 days and an eclipse duration of 11% are

given in the VSX. With such a short duration, many eclipses are likely missed in the ASAS-SN, so the light curve in Figure 3(a) does not confirm this star as an eclipsing binary. For NSVS 3242277 and NSVS 8562896 no periods are given and periodic minima are not obvious in the plots.

Figure 4 is a theoretical H-R diagram of the stars for which luminosities are listed in Table 2. Also shown are the zero-age main sequence and evolutionary tracks for 1 and 2  $M_{\odot}$  from the Yale-Potsdam models (Spada et al. 2017). Boyajian’s star is plotted using both the effective temperature from *Gaia* DR2 (filled star) and the effective temperature given by Boyajian et al. (2016, Table 3, open star).

It is striking that the candidates fall in two reasonably tight groups, one near the main sequence and the other in the red giant region. The evolutionary tracks indicate that one group consists of main-sequence or slightly evolved stars with masses similar to the Sun, and the other group may consist of evolved stars with masses near 2  $M_{\odot}$ .

The slow and rapid dippers are both distributed between the two groups. This suggests that they represent varying degrees of the same mechanism.

Two of the stars that are listed as eclipsing binaries in the VSX, NSVS 5736209 and NSVS 8562896, are in the red giant group. Thus, we consider these stars as possible dippers, but

<sup>8</sup> <http://www.aavso.org/vsx>

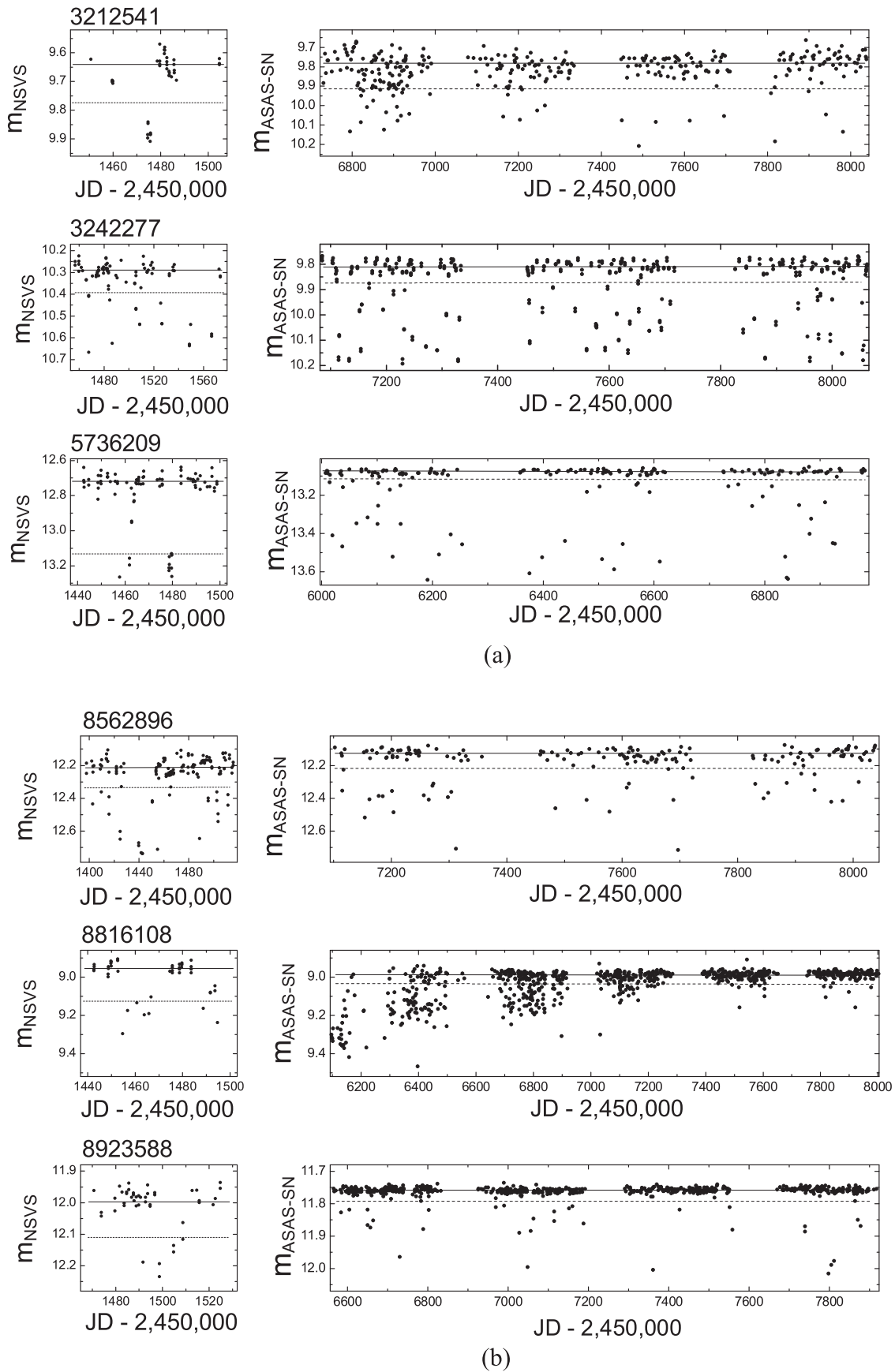


**Figure 3.** (a) Light curves for the stars classified as rapid dippers. The left-hand panels show the light curves in an interval around the strongest dip from the NSVS. The right-hand panels show the full light curves from the ASAS-SN. As in Figure 2, the continuum level and the  $3\sigma$  level are shown. (b) Light curves for rapid dippers. The layout and symbols are the same as in Figure 3(a).

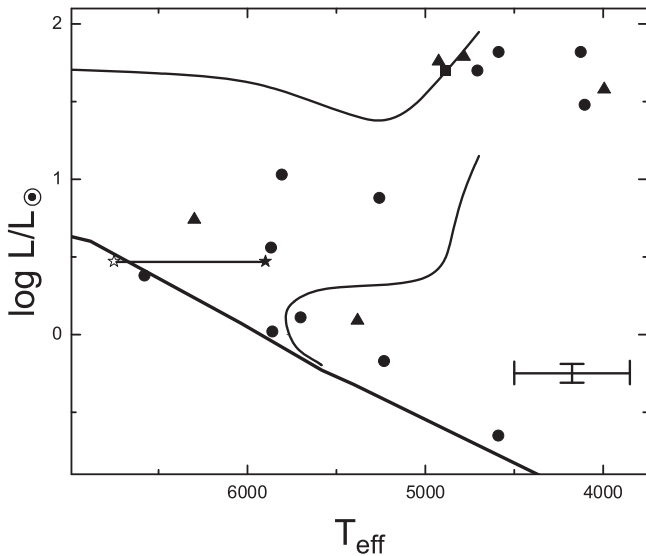


**Figure 4.** H-R diagram of the dipper candidates. Circles represent slow dippers, and triangles represent rapid dippers. Boyajian’s star is represented by stars where the filled star indicates the temperature from *Gaia* DR2 and the open star represents the temperature from Boyajian et al. (2016). The zero-age main sequence and evolutionary tracks for  $1 M_{\odot}$  and  $2 M_{\odot}$  from the Yale-Potsdam evolutionary models are also shown. The error bars in the lower right corner represent the “typical” errors (Andrae et al. 2018).

more information is needed to definitively reject the classification as eclipsing binaries. The third VSX star, NSVS 3242277, lacks a luminosity from *Gaia* and is much hotter than either of the two groups. Clearly we can reject it as a dipper candidate.

We downloaded stellar properties from *Gaia* DR2 for 2703 stars brighter than the limiting magnitude of our sample,  $V = 13.7$ . These stars were scattered about the celestial region of this survey. *Gaia* provided both the effective temperature and the luminosity for 88% of them. The lack of atmospheric parameters for the remaining 12% is largely due to limitations of the training set used for the *Gaia* Apsis software (Andrae et al. 2018).

In Figure 5 we have plotted the stars from this statistical sample as well as those from Table 2. The quadrilateral box around each of the two regions occupied by our candidates was drawn so that no candidate is closer to the nearest edge of its region than one standard deviation.

A fraction of 0.483 of the statistical sample fell within one of the boxes. Using this as the probability that a randomly drawn star from the *Gaia* DR2 would be in one of the boxes, the binomial distribution yields a probability of  $P = 0.00044$  that in randomly drawing 21 stars from the *Gaia* database, at least 18 would fall in one of the boxes. This strongly supports the conclusion that our search has successfully isolated two physically meaningful groups of stars.

The boxes in Figure 5 were only defined to test the statistical significance of the two groups; their edges do not necessarily represent physical boundaries. In particular, the hot edge of the main-sequence box falls in a region where the density of the statistical sample drops rapidly toward higher temperatures. This may affect the location of the hot boundary. However, while moving the edge of the box to a higher temperature would increase the probability  $P$ , it would not increase it enough to alter the conclusion of the previous paragraph.

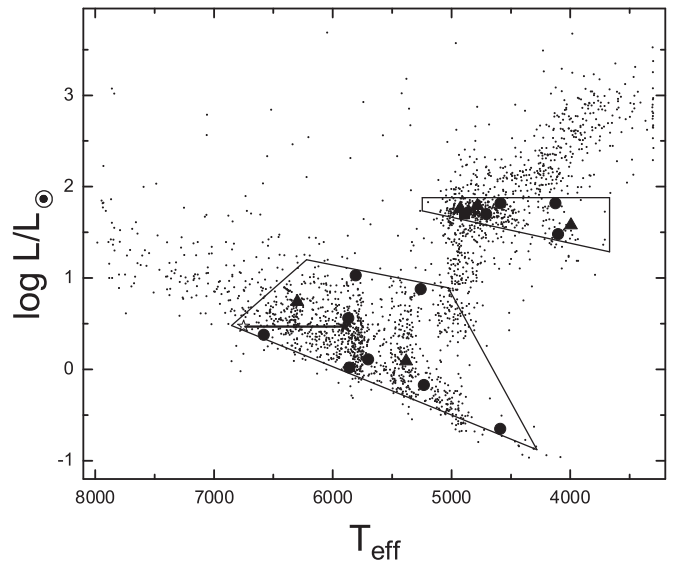


**Figure 5.** H-R diagram of the dipper candidates (same symbols as in Figure 4) and the statistical sample from *Gaia* DR2 (small dots). The two regions of the H-R diagram containing the present sample as described in Section 3.2 are enclosed by quadrilaterals.

Since Boyajian’s star falls in the main-sequence region (regardless of whether the effective temperature from *Gaia* DR2 or that from Boyajian et al. 2016 is used), these stars are very likely the analogs we sought. Whether the more luminous group is related to the main-sequence group or represents another type of object must await further observations and analysis.

#### 4. Conclusions

1. Rare stars that irregularly exhibit light-curve dips can be identified in the NSVS using the procedure described here.
2. The fact that the dipper candidates fall in two well-defined regions of the H-R diagram shows that our search has identified physically related stars.
3. Since the rapid dippers occur in both regions of the H-R diagram along with the slow dippers, it is probable that they are simply more extreme cases of the dipper phenomenon.
4. The stars in the main-sequence region are very likely analogs of Boyajian’s star. Thus, the dipping phenomenon observed in Boyajian’s star occurs among main-sequence stars with masses similar to the Sun.
5. The red giant candidates may or may not be related to the main-sequence candidates. In either case, they are interesting objects that will reward further study.
6. We encourage investigators with access to suitable facilities to monitor the dipper candidates further to confirm or reject their status as analogs to Boyajian’s star.

This publication makes use of the data from the Northern Sky Variability Survey created jointly by the Los Alamos National Laboratory and University of Michigan. The NSVS was funded by the Department of Energy, the National Aeronautics and Space Administration, and the National

Science Foundation. Data from the All Sky Automated Survey for Supernovae were used for this publication. We thank this project for making their all-sky data publicly available. This research has made use of the APASS database, located at the AAVSO website. Funding for APASS has been provided by the Robert Martin Ayers Sciences Fund. This research has made use of the SIMBAD database, operated at CDS, Strasbourg, France. This work has made use of data from the European Space Agency (ESA) mission *Gaia* (<https://www.cosmos.esa.int/gaia>), processed by the *Gaia* Data Processing and Analysis Consortium (DPAC, <https://www.cosmos.esa.int/web/gaia/dpac/consortium>). Funding for the DPAC has been provided by national institutions, in particular the institutions participating in the *Gaia* Multilateral Agreement.

#### ORCID iDs

Edward G. Schmidt  <https://orcid.org/0000-0001-7986-2962>

#### References

- Akerlof, C., Amrose, S., Balsano, R., et al. 2000, *AJ*, **119**, 1901  
 Andrae, R., Fouesneau, M., Creevey, O., et al. 2018, *A&A*, **616**, A8  
 Bodman, E. H. L., Wright, J., Boyajian, T. S., & Tyler, G. E. 2018, arXiv:1806.08842  
 Boyajian, T. S., Alonso, R., Ammerman, A., et al. 2018, *ApJL*, **853**, L8  
 Boyajian, T. S., LaCourse, D. M., Rappaport, S. A., et al. 2016, *MNRAS*, **457**, 3988  
 Cody, A. M., Stauffer, J., Baglin, A., et al. 2014, *AJ*, **147**, 82  
 Evans, D. W., Riello, M., DeAngeli, F., et al. 2018, *A&A*, **616**, A4  
 Gaia Collaboration 2016, *A&A*, **595**, A1  
 Gaia Collaboration 2018, *A&A*, **616**, A1  
 Kochanek, C. S., Shappee, B. J., Stanek, K. Z., et al. 2017, *PASP*, **129**, 104502  
 Lacourse, D. 2016, The NASA K2 Mission has yet to Observe an Analog of Tabby's Star, Zenodo, doi:10.5281/zenodo.59494  
 Schaefer, B. E. 2016, *ApJL*, **822**, L34  
 Shappee, B. J., Prieto, J. L., Grupe, D., et al. 2014, *ApJ*, **788**, 48  
 Spada, F., Demarque, P., Kim, Y.-C., Boyajian, T. S., & Brewer, J. M. 2017, *ApJ*, **838**, 161  
 Wozniak, P. R., Vestrand, W. T., Akerlof, C. W., et al. 2004, *ApJ*, **127**, 2436  
 Wright, J. T., & Sigurdsson, S. 2016, *ApJL*, **829**, L3





## Erratum: “A Search for Analogs of KIC 8462852 (Boyajian’s Star): A Proof of Concept and the First Candidates” (2019, *ApJL*, 880, L7)

Edward G. Schmidt<sup>1</sup>

Department of Physics and Astronomy, University of Nebraska, Lincoln, NE, USA

*Received 2020 August 25; published 2020 September 15*

In describing the selection of candidate stars in Section 2.1 of the published article, one criterion was inadvertently omitted and another was somewhat vague. To address this, selection criteria 1 and 2 should read as follows:

1. Multiple candidates had apparent dips on a few particular Julian dates. Since the times of dips in various stars are independent of each other, these are very likely artifacts of unknown cause. Consequently, light-curve dips near Julian dates 2,451,330, 2,451,356, 2,451,417, and 2,451,535 were ignored.
2. Any star with an NSVS light curve that resembled a possible eclipsing binary was rejected. This included any stars with dips wider than a week and stars with regularly spaced minima. Any star with an NSVS light curve resembling an intrinsic variable was rejected.

### ORCID iDs

Edward G. Schmidt <https://orcid.org/0000-0001-7986-2962>

---

<sup>1</sup> Retired. Mailing address: 685 S. La Posada Circle #3301, Green Valley, AZ 85614, USA.